Euler Diagrams, Aristotelian Diagrams and Syllogistics*

Lorenz Demey[1][0000−0002−0176−1958] and Hans Smessaert[2][0000−0002−8186−0170]

[1] Center for Logic and Philosophy of Science, KU Leuven
Kardinaal Mercierplein 2, B-3000 Leuven, Belgium
lorenz.demey@kuleuven.be
[2] Department of Linguistics, KU Leuven
Blijde-Inkomststraat 21, B-3000 Leuven, Belgium
hans.smessaert@kuleuven.be

Abstract. Euler diagrams and Aristotelian diagrams are two of the most important types of diagrams to visualize (relations between) sets. We have previously shown that Euler diagrams for two sets systematically give rise to various Aristotelian diagrams, such as classical squares of opposition. In this paper, we expand this analysis to Euler diagrams for three sets, and show that they give rise to various kinds of hexagons of opposition as well. This move from two to three sets is philosophically well-motivated and technically non-trivial. On the philosophical side, there is a connection with syllogistics, since syllogisms consist of three terms/sets. On the technical side, moving from two to three sets requires us to take the phenomenon of Boolean subtypes into account.

Keywords: Euler diagram · Aristotelian diagram · syllogistics · logical geometry · square of opposition · hexagon of opposition · syllogism.

1 Introduction

Throughout history, philosophers, mathematicians and other thinkers have devised various types of diagrams to visualize sets and the various kinds of logical relations that may hold between them. Among the most important such diagram types, there are Euler diagrams,[1] Hasse diagrams and Aristotelian diagrams.[2]

* The first author holds a Research Professorship (BOFZAP) from KU Leuven. This research was funded through the KU Leuven research project 'BITSHARE: Bitstring Semantics for Human and Artificial Reasoning' (3H190254, 2019 – 2023).

[1] An important subcase of Euler diagrams concerns the Venn diagrams. Given n sets, there are 2^n so-called zones/minimal regions. While an Euler diagram need not show each of these zones (e.g., because some zones are known to be empty anyway), a Venn diagram is required to show *all* zones, and to use shading to explicitly indicate that a given zone is known to be empty (thus also allowing us to express partial knowledge) [23, 24]. Venn diagrams can be viewed as a proper subclass of Euler diagrams, i.e., "every Venn diagram is an Euler diagram, but not every Euler diagram is a Venn diagram" [41, p. 134]. Venn diagrams will play a crucial role later in the paper.

[2] Aristotelian diagrams are traditionally considered to visualize *propositions* (and the relations between them), rather than *sets* (and the relations between them). How-

Interestingly, each of these labels turn out to be historically misleading: Euler and Hasse diagrams can already be found much earlier than the works of Leonhard Euler (1707–1783) and Helmut Hasse (1898–1979) [17, 30–32, 40]; vice versa, although Aristotelian diagrams have their theoretical roots in the logical works of Aristotle (384–322 BCE), the actual diagrams were drawn only in the 2nd century by Apuleius of Madaura [21, 34].[3] Each of these diagram types is well-understood on its own, and over the past decade, much research has been done on their various interconnections, i.e., the relation between Aristotelian and Euler diagrams [11, 16, 33], between Aristotelian and Hasse diagrams [2, 13, 15, 43], and finally, between Hasse diagrams and Euler diagrams [3, 4, 37, 38].

In this paper we will delve deeper into the interconnection between Euler and Aristotelian diagrams. Previous work in this area has been historically motivated [11, 33], but also includes a more systematic study [16]. This research has hitherto remained limited to Euler and Aristotelian diagrams for *two* sets (and their complements). The overarching goal of the present paper is to study the interaction between Euler and Aristotelian diagrams for *three* sets (and their complements). This move from two to three sets is well-motivated and non-trivial.

On the one hand, it bears emphasizing that this paper is philosophically *well-motivated*. After all, one might think that this research line is merely cumulative in nature: after previously considering (Euler and Aristotelian) diagrams for two sets, we now move to three sets, and future papers could be dedicated to four sets, five sets, and so on *ad nauseam*... However, the case of three-set diagrams is of particular interest, because these are precisely the diagrams that allow us to draw a connection with the logical system of syllogistics. Indeed, a syllogism is required to consist of precisely three terms/sets (traditionally called the 'major term', the 'minor term' and the 'middle term') [26, p. 143].[4] A typical example is the famous Barbara syllogism: 'all M are P, all S are M, so all S are P'.

On the other hand, the results presented in this paper are technically *non-trivial*. It is well-known in logical geometry that Aristotelian diagrams can have multiple Boolean subtypes [8, 14] (this will be explained later in the paper). As long as we restrict ourselves to two sets, the only Aristotelian diagrams we encounter are pairs of contradictories (PCDs), degenerate squares, and classical squares of opposition [16], which all have a unique Boolean complexity.[5] In other words, as long as we restricted ourselves to two-set diagrams, the entire issue of Boolean subtypes simply did not arise. However, once we move to three sets, we

ever, note that (i) propositions can themselves be viewed as sets, viz., sets of possible worlds [45], and (ii) Aristotelian diagrams are most naturally defined relative to some Boolean algebra, which can consist of sets just as well as of propositions [10, 16].

[3] See [5] for a dissenting voice, ascribing the square of opposition directly to Aristotle.

[4] This specific number of terms even lies at the source of one of the traditional fallacies: the *quaternio terminorum*. If one of the terms in a syllogism is ambiguous between two distinct meanings, then we are dealing with a total number of four, rather than three, terms/meanings/sets, which renders the syllogism invalid [6, p. 206ff.].

[5] In particular, PCDs always have Boolean complexity 2, classical squares of opposition always have Boolean complexity 3, and degenerate squares always have Boolean complexity 4 [8, 14].

will also encounter various hexagons of opposition, such as the Jacoby-Sesmat-Blanché (JSB) hexagon [1, 25, 42] and the unconnectedness-4 (U4) hexagon [28], which do have multiple Boolean complexities.[6] In other words, since this paper deals with three-set diagrams, it will also need to take into account the issue of Boolean subtypes, as an additional layer of complexity for our analysis.

The paper is organized as follows. Section 2 briefly recapitulates the previous work on Euler and Aristotelian diagrams for two sets, and then describes a divide and conquer strategy to move to three sets, which looks promising but is ultimately found wanting. Section 3 then presents a better strategy, based on Venn diagrams, which does allow us to systematically describe the relationship between Euler and Aristotelian diagrams for three sets. Finally, Section 4 sketches how such three-set diagrams are related to the logical system of syllogistics.

2 The Divide and Conquer Strategy

Given a domain of discourse D, it is well-known that each pair (X, Y) of non-trivial[7] sets stands in exactly one of the following seven relations [44]:

1.	contradiction (CD):	$X \cap Y = \emptyset$	and	$X \cup Y = D$,	i.e.,	$X = \overline{Y}$,
2.	contrariety (C):	$X \cap Y = \emptyset$	and	$X \cup Y \neq D$,	i.e.,	$X \subset \overline{Y}$,
3.	subcontrariety (SC):	$X \cap Y \neq \emptyset$	and	$X \cup Y = D$,	i.e.,	$X \supset \overline{Y}$,
4.	bi-implication (BI):	$X \subseteq Y$	and	$X \supseteq Y$,	i.e.,	$X = Y$,
5.	left-implication (LI):	$X \subseteq Y$	and	$X \not\supseteq Y$,	i.e.,	$X \subset Y$,
6.	right-implication (RI):	$X \not\subseteq Y$	and	$X \supseteq Y$,	i.e.,	$X \supset Y$,
7.	unconnectedness (UN):	$X \cap Y \neq \emptyset$	and	$X \cup Y \neq D$	and	
		$X \not\subseteq Y$	and	$X \not\supseteq Y$.		

In [16] we systematically investigated how the two-set Euler diagrams for each of these seven binary relations give rise to well-defined Aristotelian diagrams. For example, the Euler diagram for $LI(A, B)$ in Fig. 1(b) gives rise to the classical square of opposition in Fig. 1(e). In general, see [16, Figs. 3–9].

Let us now move from two to three sets. The results above suggest an obvious 'divide and conquer' strategy for systematically transforming three-set Euler diagrams into well-defined Aristotelian diagrams. We start from (a) any Euler diagram for three non-trivial sets A, B and C, and decompose it into subdiagrams (b) for A and B, (c) for B and C, and (d) for A and C. Next, we use the results from [16] to transform these two-set diagrams into Aristotelian diagrams (e) for A and B, (f) for B and C, and (g) for A and C, respectively. Finally, we use these last three diagrams to compose (h) a single three-set Aristotelian diagram, which corresponds precisely to the original three-set Euler diagram. As

[6] In particular, JSB hexagons can have Boolean complexities 3 and 4 [14, 36], while U4 hexagons can have have Boolean complexities 4 and 5 [12]. This issue is not restricted to hexagons of opposition; for example, Buridan octagons (which we encounter when studying four-set Euler diagrams) can have Boolean complexities 4, 5 and 6 [9].

[7] Given the domain of discourse D, a set X is said to be *non-trivial* iff $\emptyset \neq X \neq D$.

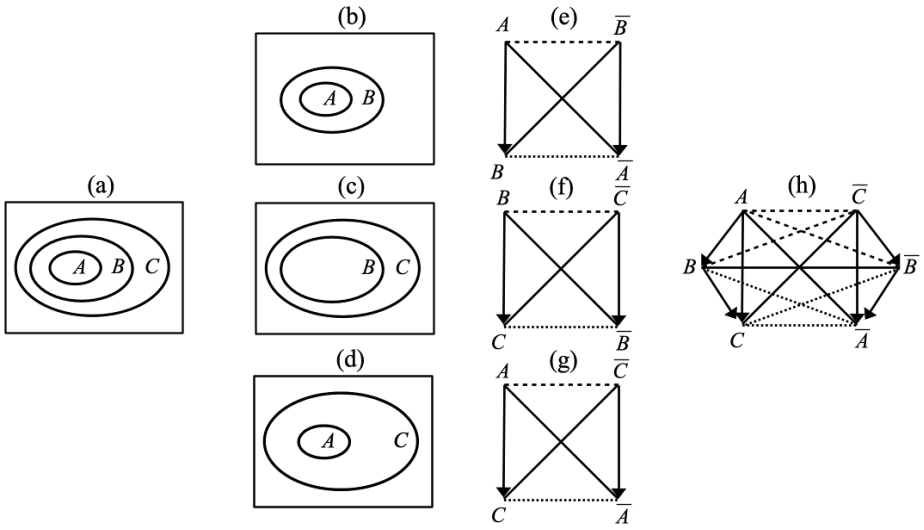

Fig. 1. Using the divide and conquer strategy to turn the Euler diagram for $A \subset B \subset C$ into a Sherwood-Czeżowski hexagon. As usual, contradiction, contrariety, subcontrariety and subalternation are visualized as resp. solid, dashed, dotted lines and arrows.

an easy example, Fig. 1 shows how the Euler diagram for $A \subset B \subset C$ gives rise to a so-called Sherwood-Czeżowski hexagon of opposition [7, 27, 29]. The labels (a–h) in Fig. 1 correspond exactly to the steps laid out before.

To do this for *all* three-set diagrams, note that (A, B) stands in exactly one of 7 relations, and similarly for (B, C) and for (A, C), so in total, we have to consider $7 \times 7 \times 7 = 343$ combinations of pairwise relations. Out of these 343 combinatorial possibilities, many turn out to be set-theoretically inconsistent; for example, if we have $LI(A, B)$ and $LI(B, C)$, then we must have $LI(A, C)$, i.e., none of the six other relations is possible for (A, C). A tedious but straightforward calculation shows that out of the 343 combinations, 102 cases represent genuine set-theoretical possibilities.[8] These 102 three-set Euler diagrams give rise to the following Aristotelian diagrams (concrete examples will be provided in Section 3; formal definitions of all these diagram types can be found in [19]):

4 pairs of contradictories,	23 Sherwood-Czeżowski hexagons,
24 classical squares of opposition,	24 unconnectedness-4 hexagons,
6 degenerate squares of opposition,	12 unconnectedness-8 hexagons,
8 Jacoby-Sesmat-Blanché hexagons,	1 unconnectedness-12 hexagon.

[8] Historically speaking, this approach is analogous to what Gergonne already did in 1817 [20, 22]. He only assumed the sets to be non-empty ($X \neq \emptyset$), rather than non-trivial ($\emptyset \neq X \neq D$), and therefore worked with 5 relations instead of 7 (using our notation, Gergonne's relations are *BI*, *LI*, *RI*, $CD \cup C$ and $SC \cup UN$). Gergonne thus considered $5 \times 5 \times 5 = 125$ combinations of pairwise relations, and showed that 54 of them represent genuine set-theoretical possibilities [20, pp. 211–213].

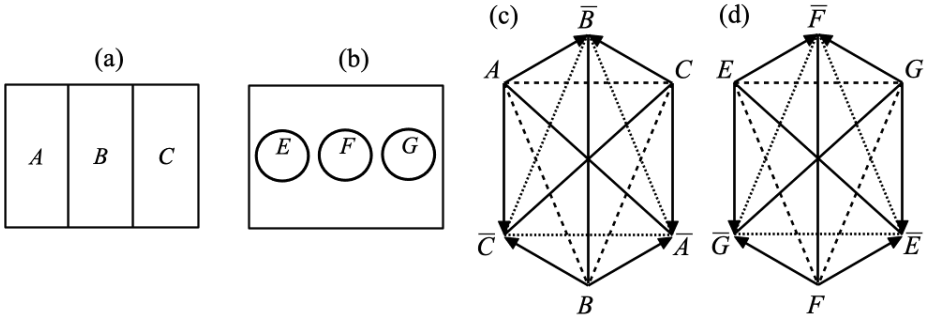

Fig. 2. Two Euler diagrams and their corresponding (strong and weak) JSB hexagons.

The divide and conquer strategy seems to work quite well. However, it faces one major technical difficulty: it does not allow us to deal with the fact that hexagons of opposition can have multiple Boolean subtypes.[9] For example, the Euler diagrams in Fig. 2(a–b) have the same configuration of Aristotelian relations among their three sets: A, B and C are pairwise contrary, and so are E, F and G. Consequently, the divide and conquer strategy transforms them into the same type of Aristotelian diagram, viz., the Jacoby-Sesmat-Blanché (JSB) hexagons in Fig. 2(c–d), respectively. However, the JSB hexagon in Fig. 2(c) is called *strong* (and said to have Boolean complexity 3), since $A \cup B \cup C = D$, whereas the JSB hexagon in Fig. 2(d) is called *weak* (and said to have Boolean complexity 4), since $E \cup F \cup G \neq D$.[10] In a truly comprehensive analysis, we want to classify not only which Euler diagrams give rise to which Aristotelian diagrams, but also which Boolean subtypes these resulting Aristotelian diagrams belong to (e.g., a JSB hexagon of Boolean complexity 3 vs 4; a U4 hexagon of Boolean complexity 4 vs 5, etc.). The divide and conquer strategy does not have the expressive power that is required for this task.

3 Using Venn Diagrams to Obtain a Complete Account

To develop a new, more fine-grained account of three-set Euler and Aristotelian diagrams, we start by having another look at the theoretical foundations of our analysis of two-set diagrams. We started Section 2 with the observation that two non-trivial sets stand in exactly one of seven relations, each of which gives rise to a well-defined Aristotelian diagram. In [16, 44], this is proved as follows:

[9] We did not encounter this issue in [16], since there, we only dealt with PCDs, classical squares and degenerate squares, which all have a unique Boolean complexity (recall Footnote 5). We did not encounter this problem in the example in Fig. 1 either, since Sherwood-Czeżowski hexagons have a unique Boolean complexity as well (viz., 4).

[10] Demey [11] already discussed a concrete historical example of this situation, without emphasizing its theoretical significance. In particular, Fig. 6(a–b) of [11, p. 196] is a three-set Euler diagram that gives rise to a *strong* JSB hexagon, while Fig. 10(a–b) of [11, p. 201] is a three-set Euler diagram that gives rise to a *weak* JSB hexagon.

1. Given two non-trivial sets A and B, we draw an Euler diagram that shows A and B as independently as possible, i.e., containing all possible intersections of $A/\overline{A}$ and $B/\overline{B}$ [44, p. 536, Fig. 4]. In the present paper, this is shown as Fig. 3(a). Note that this is a *Venn diagram*.
2. Since we start from 2 sets, the Venn diagram contains $2^2 = 4$ zones/minimal regions, viz., $A \cap B$, $A \cap \overline{B}$, $\overline{A} \cap B$ and $\overline{A} \cap \overline{B}$; cf. the labels 1–4 in Fig. 3(a).
3. Each of these 4 zones can either be empty or not, yielding $2^4 = 16$ possibilities. Out of these 16 possibilities, 9 entail that A and/or B is trivial after all, and thus have to be ruled out [44, p. 542–543, Theorem 2].
4. The remaining $16 - 9 = 7$ cases represent precisely the 7 possible relations that two non-trivial sets A and B can stand in. These can be visualized as Euler diagrams and also as Aristotelian diagrams. These 7 cases comprise 2 PCDs (for *CD* and *BI*), 4 classical squares of opposition (for *C*, *SC*, *LI* and *RI*), and 1 degenerate square of opposition (for *UN*) [16, Section 3].

This strategy via Venn diagrams can naturally be generalized from two to three sets. The major advantage of this approach is that the 'detour' via a Venn diagram allows us to take Boolean subtypes into account.[11] More concretely:

1. Given three non-trivial sets A, B and C, we draw an Euler diagram that shows A, B and C as independently as possible, i.e., containing all intersections of $A/\overline{A}$, $B/\overline{B}$ and $C/\overline{C}$. Again, this is a *Venn diagram*; cf. Fig. 3(b).
2. Since we start from 3 sets, the Venn diagram contains $2^3 = 8$ zones, viz., $A \cap B \cap C$, $A \cap B \cap \overline{C}$, $A \cap \overline{B} \cap C$, $A \cap \overline{B} \cap \overline{C}$, $\overline{A} \cap B \cap C$, $\overline{A} \cap B \cap \overline{C}$, $\overline{A} \cap \overline{B} \cap C$ and $\overline{A} \cap \overline{B} \cap \overline{C}$; cf. the labels 1–8 in Fig. 3(b).
3. Each of these 8 zones can either be empty or not, yielding $2^8 = 256$ possibilities. Another tedious but straightforward calculation shows that out of these 256 possibilities, 63 entail that A and/or B and/or C is trivial after all, and thus have to be ruled out (cf. the Appendix of this paper).
4. The remaining $256 - 63 = 193$ cases represent precisely the 193 possible configurations that three non-trivial sets A, B and C can stand in. These can be visualized as Euler diagrams and also as Aristotelian diagrams. These 193 cases comprise the following Aristotelian diagrams (cf. the Appendix):
   - 4 pairs of contradictories: all of them of Boolean complexity (BC) 2,
   - 24 classical squares of opposition: all of them of BC 3,
   - 6 degenerate squares of opposition: all of them of BC 4,
   - 16 Jacoby-Sesmat-Blanché hexagons: 8 of BC 3 and 8 of BC 4,
   - 24 Sherwood-Czeżowski hexagons: all of them of BC 4,
   - 48 unconnectedness-4 (U4) hexagons: 24 of BC 4 and 24 of BC 5,
   - 36 unconnectedness-8 (U8) hexagons: 24 of BC 5 and 12 of BC 6,
   - 35 unconnectedness-12 (U12) hexagons:
     2 of BC 4, 8 of BC 5, 16 of BC 6, 8 of BC 7, and 1 of BC 8.

[11] The tight connection that Boolean considerations have with Venn diagrams (more so than with Euler diagrams) has recently also been emphasized by Moktefi and Lemanski: "instead of orienting to *syllogistic* like *Euler* diagrams, *Venn* applied *Boolean algebra*" [35, p. 887, emphases added]. The connection between Euler diagrams, Aristotelian diagrams and syllogistics will be explored further in Section 4.

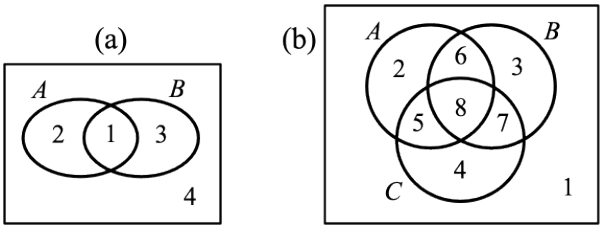

Fig. 3. Venn diagrams for two and three sets, incl. numeric labels for the zones.

All 256 cases are described in detail in the Appendix. In the remainder of this section, we will discuss examples of all (sub)types of Aristotelian diagrams and the Venn/Euler diagrams that give rise to them. For each example, we show how the Venn diagram described in the Appendix (as a configuration of 8 empty and non-empty zones) gives rise to an Euler diagram (which only shows the non-empty zones), and then determine the corresponding Aristotelian diagram. The latter's Boolean complexity corresponds to the number of non-empty zones in the Venn diagram, or equivalently, to the total number of zones in the Euler diagram.[12] In each Euler diagram, we include the zone numbers from Fig. 3(b), in order to facilitate the comparison with its description as a Venn diagram in the Appendix. Some Venn diagrams are much easier to turn into natural-looking Euler diagrams than others; in particular, in some cases we are forced to violate some of the so-called 'well-formedness properties' of Euler diagrams, such as *no multiple points* (i.e., no more than two curves should meet at a single point) and *no concurrency* (i.e., curve segments should not be concurrent) [18, 41]. In general, when a type of Aristotelian diagrams has multiple Boolean subtypes (e.g., the JSB hexagons, which can be of Boolean complexities 3 and 4), the cases with a higher Boolean complexity are easier[13] to visualize as an Euler diagram than those with a lower Boolean complexity. Therefore, in the sequence of examples below, we first discuss the case of higher Boolean complexity (e.g., a JSB hexagon of Boolean complexity 4) and only afterward that of lower Boolean complexity (e.g., a JSB hexagon of Boolean complexity 3).

PCD (of Boolean complexity 2). Case 130 from the Appendix involves zones 1 and 8 being non-empty, and all other zones being empty. It is shown as an Euler diagram in Fig. 4(a). Since zones 2 and 5 are empty, we have $A \subseteq B$, and since zones 3 and 7 are empty, we have $A \supseteq B$, and thus $A = B$, i.e., $BI(A, B)$. Completely analogously, we find $BI(B, C)$ and $BI(A, C)$. In total, this yields the PCD in Fig. 4(b).

Note that the Euler diagram in Fig. 4(a) violates *no concurrency*, since the curves for A, B and C entirely coincide with each other. This is of course a

[12] This is an interesting visual perspective on the notion of Boolean complexity, which has hitherto mainly been studied in logical geometry from a more abstract (logical/algebraic) perspective [8, 15].

[13] I.e., violating fewer well-formedness properties.

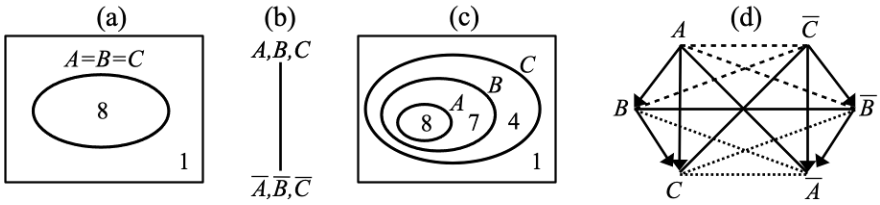

Fig. 4. Euler diagrams giving rise to a PCD and an SC hexagon.

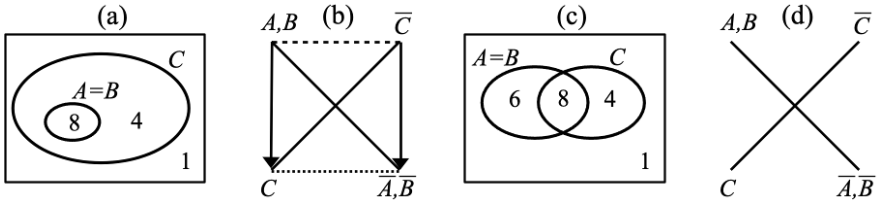

Fig. 5. Euler diagrams giving rise to a classical and a degenerate square.

direct consequence of the fact that $A = B = C$, which is also reflected in the fact that the Aristotelian diagram in Fig. 4(b) is a PCD with 3 labels at each of its vertices (rather than a hexagon with only 1 label per vertex). Analogous remarks apply to the classical and degenerate squares below (cf. Fig. 5).

SC hexagon (of Boolean complexity 4). Case 148 from the Appendix involves zones 1, 4, 7 and 8 being non-empty, and all other zones being empty. The corresponding Euler diagram is shown in Fig. 4(c), and does not violate any well-formedness properties. Since zones 2 and 5 are empty, we have $A \subseteq B$, and since zone 7 is non-empty, we have $A \not\supseteq B$, and thus $LI(A, B)$. Completely analogously, we find $LI(B, C)$ and $LI(A, C)$. In total, this yields the SC hexagon in Fig. 4(d).[14]

Classical square (of Boolean complexity 3). Case 146 from the Appendix involves zones 1, 4 and 8 being non-empty, and all other zones being empty. It is shown as an Euler diagram in Fig. 5(a). Since zones 2, 3, 5 and 7 are empty, we have $BI(A, B)$. Since zones 3 and 6 are empty, we have $B \subseteq C$, and since zone 4 is non-empty, we have $B \not\supseteq C$, and thus $LI(B, C)$. Analogousy, we find $LI(A, C)$. In total, this yields the classical square in Fig. 5(b).

Degenerate square (of Boolean complexity 4). Case 150 from the Appendix involves zones 1, 4, 6 and 8 being non-empty, and all other zones being empty. It is shown as an Euler diagram in Fig. 5(c). Since zones 2, 3, 5 and 7 are empty, we have $BI(A, B)$. Since zones 1, 4, 6 and 8 are non-empty, we find that resp. $\overline{B} \cap \overline{C}$, $\overline{B} \cap C$, $B \cap \overline{C}$ and $B \cap C$ are non-empty, and thus $UN(B, C)$. Completely analogously, we find $UN(A, C)$. In total, this yields the degenerate square in Fig. 5(d).

[14] Note that this is precisely the example that we already dealt with using the divide and conquer strategy in Section 2; in particular, cf. Fig. 1(a,h).

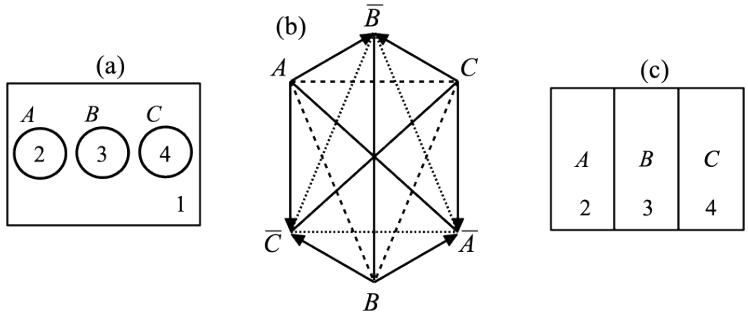

Fig. 6. Euler diagrams giving rise to JSB hexagons of Boolean complexities 4 and 3.

JSB hexagon of Boolean complexity 4. Case 241 from the Appendix involves zones 1, 2, 3 and 4 being non-empty, and all other zones being empty. The corresponding Euler diagram is shown in Fig. 6(a), and does not violate any well-formedness properties. Since zones 6 and 8 are empty, we have $A \cap B = \emptyset$, and since zones 1 and 4 are non-empty, we have $A \cup B \neq D$, and thus $C(A, B)$. Completely analogously, we also find $C(B, C)$ and $C(A, C)$. In total, this yields the JSB hexagon in Fig. 6(b).

JSB hexagon of Boolean complexity 3. Case 113 from the Appendix involves zones 2, 3 and 4 being non-empty, and all other zones being empty. The corresponding Euler diagram is shown in Fig. 6(c). This case (113) is exactly like the one before (241), except that zone 1 is now empty. This means that the Euler diagram in Fig. 6(c) can be viewed as the result of removing zone 1 from the Euler diagram in Fig. 6(a). As a result, the new Euler diagram in Fig. 6(c) violates the wellformedness property of *no concurrency*, since the curves for A and B (and those for B and C) are partially concurrent. Just like in the previous case, we find $C(A, B)$, $C(B, C)$ and $C(A, C)$, and thus again obtain the JSB hexagon in Fig. 6(b).[15]

U4 hexagon of Boolean complexity 5. Case 249 from the Appendix involves zones 1, 2, 3, 4 and 5 being non-empty, and all other zones being empty. The corresponding Euler diagram is shown in Fig. 7(a), and does not violate any well-formedness properties. Since zones 6 and 8 are empty, we have $A \cap B = \emptyset$, and since zones 1 and 4 are non-empty, we have $A \cup B \neq D$, and thus $C(A, B)$. Completely analogously, we also find $C(B, C)$. Since zones 1, 2, 4 and 5 are non-empty, we find that resp. $\overline{A} \cap \overline{C}$, $A \cap \overline{C}$, $\overline{A} \cap C$ and $A \cap C$ are non-empty, and thus $UN(A, C)$. In total, this yields the U4 hexagon in Fig. 7(b).

U4 hexagon of Boolean complexity 4. Case 121 from the Appendix involves zones 2, 3, 4 and 5 being non-empty, and all other zones being empty. The

[15] Note that the JSB hexagons of Boolean complexities 4 and 3 that we have just considered are precisely those that were already used in Section 2 to demonstrate the expressive inadequacy of the divide and conquer strategy; in particular; cf. Fig. 2.

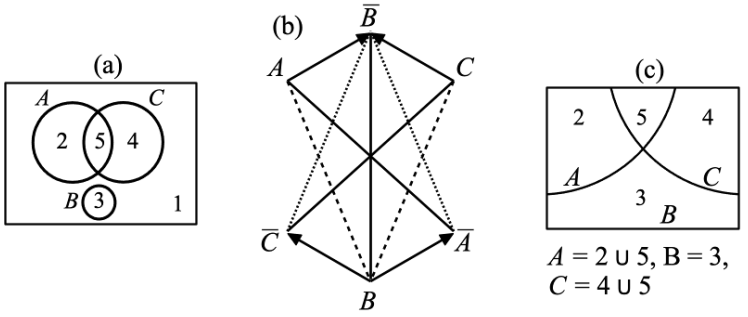

Fig. 7. Euler diagrams giving rise to U4 hexagons of Boolean complexities 5 and 4.

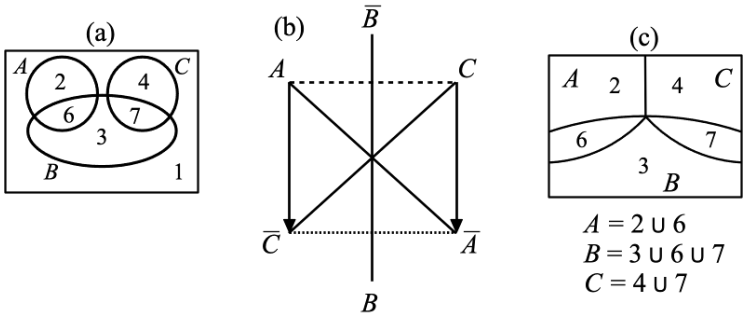

Fig. 8. Euler diagrams giving rise to U8 hexagons of Boolean complexities 6 and 5.

corresponding Euler diagram is shown in Fig. 7(c). This case (121) is exactly like the one before (249), except that zone 1 is now empty. This means that the Euler diagram in Fig. 7(c) can be viewed as the result of removing zone 1 from the Euler diagram in Fig. 7(a). As a result, the new Euler diagram in Fig. 7(c) violates the well-formedness property of *no concurrency*, since the curves for A and B (and those for B and C) are partially concurrent. Just like in the previous case, we find $C(A, B)$, $C(B, C)$ and $UN(A, C)$, and thus again obtain the U4 hexagon in Fig. 7(b).

U8 hexagon of Boolean complexity 6. Case 247 from the Appendix involves zones 1, 2, 3, 4, 6 and 7 being non-empty, and all other zones being empty. The corresponding Euler diagram is shown in Fig. 8(a), and does not violate any well-formedness properties. Since zones 2, 3, 4 and 6 are non-empty, we find that resp. $A \cap \overline{B}$, $\overline{A} \cap B$, $\overline{A} \cap \overline{B}$ and $A \cap B$ are non-empty, and thus $UN(A, B)$. Completely analogously, we also find $UN(B, C)$. Finally, since zones 5 and 8 are empty, we have $A \cap C = \emptyset$, and since the other zones are non-empty, we have $A \cup C \neq D$, and thus $C(A, C)$. In total, this yields the U8 hexagon in Fig. 8(b).

U8 hexagon of Boolean complexity 5. Case 119 from the Appendix involves zones 2, 3, 4, 6 and 7 being non-empty, and all other zones being empty. The

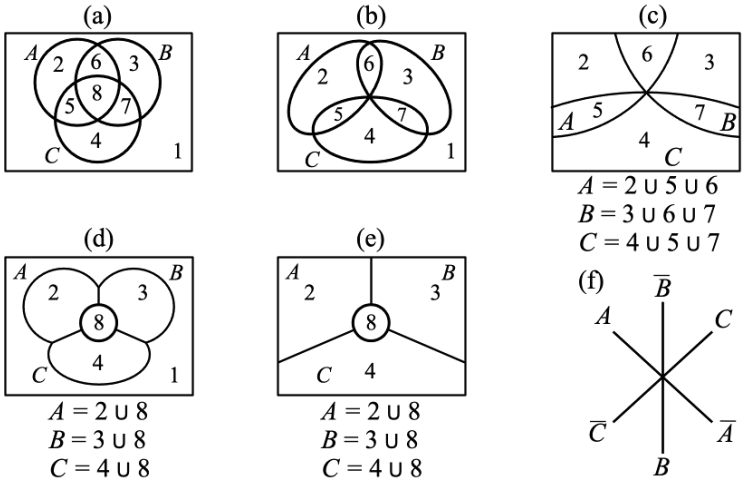

Fig. 9. Euler diagrams giving rise to U12 hexagons of BC 8, 7, 6, 5 and 4.

corresponding Euler diagram is shown in Fig. 8(c). This case (119) is exactly like the one before (247), except that zone 1 is now empty. This means that the Euler diagram in Fig. 8(c) can be viewed as the result of removing zone 1 from the Euler diagram in Fig. 8(a). As a result, the new Euler diagram in Fig. 8(c) violates both the well-formedness property of *no multiple points* (since the curves for A, B and C all meet at a single point) and that of *no concurrency* (since the curves for A and C are partially concurrent). Just like in the previous case, we find $UN(A, B)$, $UN(B, C)$ and $C(A, C)$, and thus again obtain the U8 hexagon in Fig. 8(b).

U12 hexagon of Boolean complexity 8. Case 256 from the Appendix involves *all* zones being non-empty. Consequently, the corresponding Euler diagram, as shown in Fig. 9(a), simply *is* a Venn diagram, and does not violate any well-formedness properties. Since zones 2, 3, 4 and 6 are non-empty, we find that resp. $A \cap \overline{B}$, $\overline{A} \cap B$, $\overline{A} \cap \overline{B}$ and $A \cap B$ are non-empty, and thus $UN(A, B)$. Completely analogously, we also find $UN(B, C)$ and $UN(A, C)$. In total, this yields the U12 hexagon in Fig. 9(f).

U12 hexagon of Boolean complexity 7. Case 255 from the Appendix involves all zones being non-empty, except for zone 8. The corresponding Euler diagram is shown in Fig. 9(b), and can be viewed as the result of removing zone 8 from the Euler/Venn diagram in Fig. 9(a). As a result, the new Euler diagram in Fig. 9(b) violates the well-formedness property of *no multiple points*, since the curves for A, B and C all meet at a single point. Just like in the previous case, we find $UN(A, B)$, $UN(B, C)$ and $UN(A, C)$, and thus again obtain the U12 hexagon in Fig. 9(f).

U12 hexagon of Boolean complexity 6. Case 127 from the Appendix involves all zones being non-empty, except for zones 1 and 8. The corresponding Euler diagram is shown in Fig. 9(c), and can be viewed as the result of

removing zone 1 from the Euler diagram in Fig. 9(b), or alternatively, as the result of removing zones 1 and 8 from the Euler/Venn diagram in Fig. 9(a). As a result, the new Euler diagram in Fig. 9(c) violates the well-formedness property of *no multiple points*, since the curves for A, B and C all meet at a single point. Just like in the previous case, we find $UN(A, B)$, $UN(B, C)$ and $UN(A, C)$, and thus again obtain the U12 hexagon in Fig. 9(f).

U12 hexagon of Boolean complexity 5. Case 242 from the Appendix involves all zones being non-empty, except for zones 5, 6 and 7. The corresponding Euler diagram is shown in Fig. 9(d), and can be viewed as the result of simultaneously removing zones 5, 6 and 7 from the Euler/Venn diagram in Fig. 9(a). As a result, the new Euler diagram in Fig. 9(d) violates the well-formedness property of *no concurrency*, since the curves for A and B (and those for B and C, and those for A and C) are partially concurrent. We still have $UN(A, B)$, $UN(B, C)$ and $UN(A, C)$, and thus again obtain the U12 hexagon in Fig. 9(f).

U12 hexagon of Boolean complexity 4. Case 114 from the Appendix involves zones 2, 3, 4 and 8 being non-empty, and all other zones being empty. The corresponding Euler diagram is shown in Fig. 9(e), and can be viewed as the result of removing zone 1 from the Euler diagram in Fig. 9(d), or alternatively, as the result of removing zones 1, 5, 6 and 7 from the Euler/Venn diagram in Fig. 9(a). As a result, the new Euler diagram in Fig. 9(e) violates the well-formedness property of *no concurrency*, since the curves for A and B (and those for B and C, and those for A and C) are partially concurrent. We still have $UN(A, B)$, $UN(B, C)$ and $UN(A, C)$, and thus again obtain the U12 hexagon in Fig. 9(f).

To conclude this systematic discussion, it is worth highlighting how intricately (the examples of) the various Boolean subtypes of U12 hexagons are related to each other. Starting from the Euler/Venn diagram in Fig. 9(a), which is of Boolean complexity 8, we can either (i) remove zone 8 (corresponding to the triple intersection $A \cap B \cap C$) to obtain the Euler diagram in Fig. 9(b), which is of BC 7, or (ii) remove zones 5, 6 and 7 (corresponding to the 'binary' intersections $A \cap B \cap \overline{C}$, $A \cap \overline{B} \cap C$ and $\overline{A} \cap B \cap C$) to obtain the Euler diagram in Fig. 9(d), which is of BC 5. In either scenario, we can subsequently remove zone 1: in scenario (i) this takes us from Fig. 9(b) to Fig. 9(c), which is of BC 6; in scenario (ii), this takes us from Fig. 9(d) to Fig. 9(e), which is of BC 4.

4 Outlook: Aristotelian Diagrams and Syllogistics

It is quite common to explain syllogistics, and in particular the validity of specific syllogisms, using Euler diagrams [26, p. 141ff.] or Venn diagrams; cf. [6, p. 197ff.], [26, p. 207ff.] and [39, p. 74ff.]. In light of the results from the previous section, we are now in a position to draw a connection with Aristotelian diagrams as well. For reason of space, we do not provide a detailed introduction to the system of syllogistics (using the traditional terminology of 'mood', 'figure', etc.), which can be found in many traditional as well as symbolic logic textbooks [6, 26, 39].

The semantic/model-theoretic validity of an argument is defined as *truth preservation*: every model that makes all premises true, also makes the conclusion true. In the case of a syllogism, which has precisely three terms (distributed over two premises and one conclusion), this universal quantification over models can be replaced with a universal quantification over the 256 Venn diagrams (and their corresponding Euler and Aristotelian diagrams) described in the Appendix. A syllogism is thus valid iff every diagram that makes its two premises true, also makes its conclusion true. As an example, let's consider the famous Barbara syllogism: 'all M are P, all S are M, so all S are P'. The first premise is true whenever $BI(M,P)$ or $LI(M,P)$, and similarly, the second premise is true whenever $BI(S,M)$ or $LI(S,M)$. We thus have to consider four cases in total:

***BI(M,P)* and *BI(S,M)*.** In this case, it follows that $BI(S,P)$, and thus the conclusion ('all S are P') is also true. This is case 130 from the Appendix, which gives rise to a PCD; cf. Fig. 4(a–b).[16]

***LI(M,P)* and *BI(S,M)*.** In this case, it follows that $LI(S,P)$, and thus the conclusion is also true. This is case 146 from the Appendix, which gives rise to a classical square of opposition; cf. Fig. 5(a–b).

***BI(M,P)* and *LI(S,M)*.** In this case, it follows that $LI(S,P)$, and thus the conclusion is also true. This is case 132 from the Appendix, which gives rise to a classical square of opposition.

***LI(M,P)* and *LI(S,M)*.** In this case, it follows that $LI(S,P)$, and thus the conclusion is also true. This is case 148 from the Appendix, which gives rise to a Sherwood-Czeżowski hexagon; cf. Fig. 4(c–d).

Since all diagrams which make the two premises of Barbara true, also make its conclusion true, we find that Barbara is valid. Furthermore, we observe that this validity is exhibited by 1 PCD, 2 classical squares and 1 SC hexagon (for the four corresponding Euler diagrams, also see [26, p. 203]). Using the ranking numbers from the Appendix, we can write $[\![\text{Barbara}]\!] = \{130, 132, 146, 148\}$.

Continuing along this way, we obtain a diagrammatic semantics for syllogistics, which maps every syllogism σ onto a set $[\![\sigma]\!] \subseteq \{1, 2, \ldots, 255, 256\}$. In ongoing research, we are investigating the properties of this semantics. For example, one can show that if there is a U12 hexagon in $[\![\sigma]\!]$, then σ is invalid. This establishes an important connection between unconnectedness (as a relation between propositions [44]) and invalidity (as a property of arguments).

References

1. Blanché, R.: Sur l'opposition des concepts. Theoria **19**, 89–130 (1953)
2. Bolz, R.: Logical diagrams, visualization criteria, and Boolean algebras. In: Beziau, J.Y., Vandoulakis, I. (eds.) The Exoteric Square of Opposition, pp. 195–224. Springer (2022)

[16] When referring to Figs. 4–5 in this context, all occurrences of the set labels 'A', 'B' and 'C' in those figures should be read as resp. 'S', 'M' and 'P'.

3. Bourou, D., Schorlemmer, M., Plaza, E.: Euler vs Hasse diagrams for reasoning about sets: A cognitive approach. In: Giardino, V., et al. (eds.) Diagrammatic Representation and Inference, pp. 151–167. LNCS 13462, Springer (2022)
4. Bourou, D., Schorlemmer, M., Plaza, E.: An image-schematic analysis of Hasse and Euler diagrams. In: Hedblom, M.M., Kutz, O. (eds.) ISD7 – Proceedings of the 7th Image Schema Day 2023, pp. 1–8. CEUR-WS 3511, CEUR-WS (2023)
5. Christensen, R.: The first square of opposition. Phronesis **68**, 371–383 (2023)
6. Copi, I.M., Cohen, C.: Introduction to Logic. Eighth Edition. Prentice Hall (1990)
7. Czeżowski, T.: On certain peculiarities of singular propositions. Mind **64**, 392–395 (1955)
8. Demey, L.: Computing the maximal Boolean complexity of families of Aristotelian diagrams. Journal of Logic and Computation **28**, 1323–1339 (2018)
9. Demey, L.: Boolean considerations on John Buridan's octagons of opposition. History and Philosophy of Logic **40**, 116–134 (2019)
10. Demey, L.: Metalogic, metalanguage and logical geometry. Logique et Analyse **248**, 453–478 (2019)
11. Demey, L.: From Euler diagrams in Schopenhauer to Aristotelian diagrams in logical geometry. In: Lemanski, J. (ed.) Language, Logic, and Mathematics in Schopenhauer, pp. 181–205. Springer (2020)
12. Demey, L., Erbas, A.: Boolean subtypes of the U4 hexagon of opposition. Axioms **13**, 1–20 (2024)
13. Demey, L., Smessaert, H.: The relationship between Aristotelian and Hasse diagrams. In: Dwyer, T., Purchase, H., Delaney, A. (eds.) Diagrammatic Representation and Inference, pp. 213–227. LNCS 8578, Springer (2014)
14. Demey, L., Smessaert, H.: Combinatorial bitstring semantics for arbitrary logical fragments. Journal of Philosophical Logic **47**, 325–363 (2018)
15. Demey, L., Smessaert, H.: Geometric and cognitive differences between Aristotelian diagrams for the Boolean algebra $\mathbb{B}_4$. Annals of Mathematics and Artificial Intelligence **83**, 185–208 (2018)
16. Demey, L., Smessaert, H.: From Euler diagrams to Aristotelian diagrams. In: Giardino, V., et al. (eds.) Diagrammatic Representation and Inference, pp. 279–295. LNCS 13462, Springer (2022)
17. Edwards, A.W.F.: An eleventh-century Venn diagram. BSHM Bulletin **21**, 119–121 (2006)
18. Fish, A., Khazaei, B., Roast, C.: User-comprehension of Euler diagrams. Journal of Visual Languages & Computing **22**, 340–354 (2011)
19. Frijters, S., Demey, L.: The modal logic of Aristotelian diagrams. Axioms **12**, 1–26 (2023)
20. Gergonne, J.D.: Essai de dialectique rationelle. Annales des Mathématiques Pures et Appliquées **7**, 189–228 (1817)
21. Geudens, C., Demey, L.: On the Aristotelian roots of the modal square of opposition. Logique et Analyse **255**, 313–348 (2021)
22. Giard, L.: La "Dialectique rationnelle" de Gergonne. Revue d'Histoire des Sciences **25**, 97–124 (1972)
23. Hammer, E., Shin, S.J.: Euler's visual logic. History and Philosophy of Logic **19**, 1–29 (1998)
24. Howse, J., Stapleton, G., Flower, J., Taylor, J.: Corresponding regions in Euler diagrams. In: Hegarty, M., et al. (eds.) Diagrammatic Representation and Inference, pp. 76–90. LNCS 2317, Springer (2002)
25. Jacoby, P.: A triangle of opposites for types of propositions in Aristotelian logic. New Scholasticism **24**, 32–56 (1950)

26. Keynes, J.N.: Studies and Exercises in Formal Logic. MacMillan (1884)
27. Khomskii, Y.: William of Sherwood, singular propositions and the hexagon of opposition. In: Béziau, J.Y., Payette, G. (eds.) New Perspectives on the Square of Opposition. Peter Lang, Bern (2011)
28. Kraszewski, Z.: Logika stosunków zakresowych. Studia Logica **4**, 63–116 (1956)
29. Kretzmann, N.: William of Sherwood's Introduction to Logic. Minnesota Archive Editions (1966)
30. Lemanski, J.: Periods in the use of Euler-type diagrams. Acta Baltica Historiae et Philosophiae Scientiarum **5**, 50–69 (2017)
31. Lemanski, J.: Logic diagrams in the Weigel and Weise circles. History and Philosophy of Logic **39**, 3–28 (2018)
32. Lemanski, J.: Euler-type diagrams and the quantification of the predicate. Journal of Philosophical Logic **49**, 401–416 (2020)
33. Lemanski, J., Demey, L.: Schopenhauer's partition diagrams and logical geometry. In: Basu, A., et al. (eds.) Diagrammatic Representation and Inference. pp. 149–165. LNCS 12909, Springer (2021)
34. Londey, D., Johanson, C.: Apuleius and the square of opposition. Phronesis **29**, 165–173 (1984)
35. Moktefi, A., Lemanski, J.: On the origin of Venn diagrams. Axiomathes **32 (Suppl 3)**, S887–S900 (2022)
36. Pellissier, R.: Setting n-opposition. Logica Universalis **2**(2), 235–263 (2008)
37. Priss, U.: A semiotic-conceptual analysis of Euler and Hasse diagrams. In: Pietarinen, A.V., et al. (eds.) Diagrammatic Representation and Inference, pp. 515–519. LNCS 12169, Springer (2020)
38. Priss, U.: Set visualisations with Euler and Hasse diagrams. In: Cochez, M., et al. (eds.) Graph Structures for Knowledge Representation and Reasoning (GKR 2020), pp. 72–83. LNCS 12640, Springer (2021)
39. Quine, W.V.O.: Methods of Logic (Revised Edition). Holt, Rinehart and Winston (1966)
40. Rival, I.: The diagram. In: Rival, I. (ed.) Graphs and Order: The Role of Graphs in the Theory of Ordered Sets and Its Applications, pp. 103–133. Springer (1985)
41. Rodgers, P.: A survey of Euler diagrams. Journal of Visual Languages & Computing **25**, 134–155 (2014)
42. Sesmat, A.: Logique II. Hermann (1951)
43. Smessaert, H.: On the 3D visualisation of logical relations. Logica Universalis **3**, 303–332 (2009)
44. Smessaert, H., Demey, L.: Logical geometries and information in the square of opposition. Journal of Logic, Language and Information **23**, 527–565 (2014)
45. Stalnaker, R.C.: Inquiry. MIT Press (1984)

Appendix: Description of All 256 Cases

The table below describes all $2^8 = 256$ cases, as computed in Section 3. Each case is described as follows: a ranking number (from 1 to 256) that uniquely identifies the case, a description of which zones/minimal regions (cf. the numbering in Fig. 3(b)) are empty (indicated by '$\circ$') and which are non-empty (indicated by '$\bullet$'), and finally, a classification of the corresponding Aristotelian diagram. If a case entails that at least one of the sets A, B or C is trivial (i.e., equal to $\emptyset$ or to the domain D), this is indicated by '—'. The Boolean complexity of each case can simply be determined by counting the number of $\bullet$'s in the case description.

	1	2	3	4	5	6	7	8	diagram
1	○	○	○	○	○	○	○	○	—
2	○	○	○	○	○	○	○	●	—
3	○	○	○	○	○	○	●	○	—
4	○	○	○	○	○	○	●	●	—
5	○	○	○	○	○	●	○	○	—
6	○	○	○	○	○	●	○	●	—
7	○	○	○	○	○	●	●	○	—
8	○	○	○	○	○	●	●	●	—
9	○	○	○	○	●	○	○	○	—
10	○	○	○	○	●	○	○	●	—
11	○	○	○	○	●	○	●	○	—
12	○	○	○	○	●	○	●	●	—
13	○	○	○	○	●	●	○	○	—
14	○	○	○	○	●	●	○	●	—
15	○	○	○	○	●	●	●	○	JSB hex.
16	○	○	○	○	●	●	●	●	JSB hex.
17	○	○	○	●	○	○	○	○	—
18	○	○	○	●	○	○	○	●	—
19	○	○	○	●	○	○	●	○	—
20	○	○	○	●	○	○	●	●	—
21	○	○	○	●	○	●	○	○	PCD
22	○	○	○	●	○	●	○	●	class. sq.
23	○	○	○	●	○	●	●	○	class. sq.
24	○	○	○	●	○	●	●	●	SC hex.
25	○	○	○	●	●	○	○	○	—
26	○	○	○	●	●	○	○	●	—
27	○	○	○	●	●	○	●	○	—
28	○	○	○	●	●	○	●	●	—
29	○	○	○	●	●	●	○	○	class. sq.
30	○	○	○	●	●	●	○	●	SC hex.
31	○	○	○	●	●	●	●	○	U4 hex.
32	○	○	○	●	●	●	●	●	U4 hex.
33	○	○	●	○	○	○	○	○	—
34	○	○	●	○	○	○	○	●	—
35	○	○	●	○	○	○	●	○	—
36	○	○	●	○	○	○	●	●	—
37	○	○	●	○	○	●	○	○	—
38	○	○	●	○	○	●	○	●	—
39	○	○	●	○	○	●	●	○	—
40	○	○	●	○	○	●	●	●	—
41	○	○	●	○	●	○	○	○	PCD
42	○	○	●	○	●	○	○	●	class. sq.
43	○	○	●	○	●	○	●	○	class. sq.
44	○	○	●	○	●	○	●	●	SC hex.
45	○	○	●	○	●	●	○	○	class. sq.
46	○	○	●	○	●	●	○	●	SC hex.
47	○	○	●	○	●	●	●	○	U4 hex.
48	○	○	●	○	●	●	●	●	U4 hex.
49	○	○	●	●	○	○	○	○	—
50	○	○	●	●	○	○	○	●	JSB hex.
51	○	○	●	●	○	○	●	○	—
52	○	○	●	●	○	○	●	●	JSB hex.
53	○	○	●	●	○	●	○	○	class. sq.
54	○	○	●	●	○	●	○	●	U4 hex.
55	○	○	●	●	○	●	●	○	SC hex.
56	○	○	●	●	○	●	●	●	U4 hex.
57	○	○	●	●	●	○	○	○	class. sq.
58	○	○	●	●	●	○	○	●	U4 hex.
59	○	○	●	●	●	○	●	○	SC hex.
60	○	○	●	●	●	○	●	●	U4 hex.
61	○	○	●	●	●	●	○	○	degen. sq.
62	○	○	●	●	●	●	○	●	U8 hex.
63	○	○	●	●	●	●	●	○	U8 hex.
64	○	○	●	●	●	●	●	●	U8 hex.
65	○	●	○	○	○	○	○	○	—
66	○	●	○	○	○	○	○	●	—
67	○	●	○	○	○	○	●	○	PCD
68	○	●	○	○	○	○	●	●	class. sq.
69	○	●	○	○	○	●	○	○	—
70	○	●	○	○	○	●	○	●	—
71	○	●	○	○	○	●	●	○	class. sq.
72	○	●	○	○	○	●	●	●	SC hex.
73	○	●	○	○	●	○	○	○	—
74	○	●	○	○	●	○	○	●	—
75	○	●	○	○	●	○	●	○	class. sq.
76	○	●	○	○	●	○	●	●	SC hex.
77	○	●	○	○	●	●	○	○	—
78	○	●	○	○	●	●	○	●	—
79	○	●	○	○	●	●	●	○	U4 hex.
80	○	●	○	○	●	●	●	●	U4 hex.
81	○	●	○	●	○	○	○	○	—
82	○	●	○	●	○	○	○	●	JSB hex.
83	○	●	○	●	○	○	●	○	class. sq.
84	○	●	○	●	○	○	●	●	U4 hex.
85	○	●	○	●	○	●	○	○	class. sq.
86	○	●	○	●	○	●	○	●	U4 hex.
87	○	●	○	●	○	●	●	○	degen. sq.
88	○	●	○	●	○	●	●	●	U8 hex.
89	○	●	○	●	●	○	○	○	—
90	○	●	○	●	●	○	○	●	JSB hex.
91	○	●	○	●	●	○	●	○	SC hex.
92	○	●	○	●	●	○	●	●	U4 hex.
93	○	●	○	●	●	●	○	○	SC hex.
94	○	●	○	●	●	●	○	●	U4 hex.
95	○	●	○	●	●	●	●	○	U8 hex.
96	○	●	○	●	●	●	●	●	U8 hex.
97	○	●	●	○	○	○	○	○	—
98	○	●	●	○	○	○	○	●	JSB hex.
99	○	●	●	○	○	○	●	○	class. sq.
100	○	●	●	○	○	○	●	●	U4 hex.
101	○	●	●	○	○	●	○	○	—
102	○	●	●	○	○	●	○	●	JSB hex.
103	○	●	●	○	○	●	●	○	SC hex.
104	○	●	●	○	○	●	●	●	U4 hex.
105	○	●	●	○	●	○	○	○	class. sq.
106	○	●	●	○	●	○	○	●	U4 hex.
107	○	●	●	○	●	○	●	○	degen. sq.
108	○	●	●	○	●	○	●	●	U8 hex.
109	○	●	●	○	●	●	○	○	SC hex.
110	○	●	●	○	●	●	○	●	U4 hex.
111	○	●	●	○	●	●	●	○	U8 hex.
112	○	●	●	○	●	●	●	●	U8 hex.
113	○	●	●	●	○	○	○	○	JSB hex.
114	○	●	●	●	○	○	○	●	U12 hex.
115	○	●	●	●	○	○	●	○	U4 hex.
116	○	●	●	●	○	○	●	●	U12 hex.
117	○	●	●	●	○	●	○	○	U4 hex.
118	○	●	●	●	○	●	○	●	U12 hex.
119	○	●	●	●	○	●	●	○	U8 hex.
120	○	●	●	●	○	●	●	●	U12 hex.
121	○	●	●	●	●	○	○	○	U4 hex.
122	○	●	●	●	●	○	○	●	U12 hex.
123	○	●	●	●	●	○	●	○	U8 hex.
124	○	●	●	●	●	○	●	●	U12 hex.
125	○	●	●	●	●	●	○	○	U8 hex.
126	○	●	●	●	●	●	○	●	U12 hex.
127	○	●	●	●	●	●	●	○	U12 hex.
128	○	●	●	●	●	●	●	●	U12 hex.
129	●	○	○	○	○	○	○	○	—
130	●	○	○	○	○	○	○	●	PCD
131	●	○	○	○	○	○	●	○	—
132	●	○	○	○	○	○	●	●	class. sq.
133	●	○	○	○	○	●	○	○	—
134	●	○	○	○	○	●	○	●	class. sq.
135	●	○	○	○	○	●	●	○	JSB hex.
136	●	○	○	○	○	●	●	●	U4 hex.
137	●	○	○	○	●	○	○	○	—
138	●	○	○	○	●	○	○	●	class. sq.
139	●	○	○	○	●	○	●	○	JSB hex.
140	●	○	○	○	●	○	●	●	U4 hex.
141	●	○	○	○	●	●	○	○	JSB hex.
142	●	○	○	○	●	●	○	●	U4 hex.
143	●	○	○	○	●	●	●	○	U12 hex.
144	●	○	○	○	●	●	●	●	U12 hex.
145	●	○	○	●	○	○	○	○	—
146	●	○	○	●	○	○	○	●	class. sq.
147	●	○	○	●	○	○	●	○	—
148	●	○	○	●	○	○	●	●	SC hex.
149	●	○	○	●	○	●	○	○	class. sq.
150	●	○	○	●	○	●	○	●	degen.sq.
151	●	○	○	●	○	●	●	○	U4 hex.
152	●	○	○	●	○	●	●	●	U8 hex.
153	●	○	○	●	●	○	○	○	—
154	●	○	○	●	●	○	○	●	SC hex.
155	●	○	○	●	●	○	●	○	JSB hex.
156	●	○	○	●	●	○	●	●	U4 hex.
157	●	○	○	●	●	●	○	○	U4 hex.
158	●	○	○	●	●	●	○	●	U8 hex.
159	●	○	○	●	●	●	●	○	U12 hex.
160	●	○	○	●	●	●	●	●	U12 hex.
161	●	○	●	○	○	○	○	○	—
162	●	○	●	○	○	○	○	●	class. sq.
163	●	○	●	○	○	○	●	○	—
164	●	○	●	○	○	○	●	●	SC hex.
165	●	○	●	○	○	●	○	○	—
166	●	○	●	○	○	●	○	●	SC hex.
167	●	○	●	○	○	●	●	○	JSB hex.
168	●	○	●	○	○	●	●	●	U4 hex.
169	●	○	●	○	●	○	○	○	class. sq.
170	●	○	●	○	●	○	○	●	degen. sq.
171	●	○	●	○	●	○	●	○	U4 hex.
172	●	○	●	○	●	○	●	●	U8 hex.
173	●	○	●	○	●	●	○	○	U4 hex.
174	●	○	●	○	●	●	○	●	U8 hex.
175	●	○	●	○	●	●	●	○	U12 hex.
176	●	○	●	○	●	●	●	●	U12 hex.
177	●	○	●	●	○	○	○	○	—
178	●	○	●	●	○	○	○	●	U4 hex.
179	●	○	●	●	○	○	●	○	—
180	●	○	●	●	○	○	●	●	U4 hex.
181	●	○	●	●	○	●	○	○	SC hex.
182	●	○	●	●	○	●	○	●	U8 hex.
183	●	○	●	●	○	●	●	○	U4 hex.
184	●	○	●	●	○	●	●	●	U8 hex.
185	●	○	●	●	○	○	○	○	SC hex.
186	●	○	●	●	○	○	○	●	U8 hex.
187	●	○	●	●	○	○	●	○	U4 hex.
188	●	○	●	●	○	○	●	●	U8 hex.
189	●	○	●	●	●	○	○	○	U8 hex.
190	●	○	●	●	●	○	○	●	U12 hex.
191	●	○	●	●	●	○	●	○	U12 hex.
192	●	○	●	●	●	○	●	●	U12 hex.
193	●	●	○	○	○	○	○	○	—
194	●	●	○	○	○	○	○	●	class. sq.
195	●	●	○	○	○	○	●	○	class. sq.
196	●	●	○	○	○	○	●	●	degen. sq.
197	●	●	○	○	○	●	○	○	—
198	●	●	○	○	○	●	○	●	SC hex.
199	●	●	○	○	○	●	●	○	U4 hex.
200	●	●	○	○	○	●	●	●	U8 hex.
201	●	●	○	○	●	○	○	○	—
202	●	●	○	○	●	○	○	●	SC hex.
203	●	●	○	○	●	○	●	○	U4 hex.
204	●	●	○	○	●	○	●	●	U8 hex.
205	●	●	○	○	●	●	○	○	JSB hex.
206	●	●	○	○	●	●	○	●	U4 hex.
207	●	●	○	○	●	●	●	○	U12 hex.
208	●	●	○	○	●	●	●	●	U12 hex.
209	●	●	○	●	○	○	○	○	—
210	●	●	○	●	○	○	○	●	U4 hex.
211	●	●	○	●	○	○	●	○	SC hex.
212	●	●	○	●	○	○	●	●	U8 hex.
213	●	●	○	●	○	●	○	○	SC hex.
214	●	●	○	●	○	●	○	●	U8 hex.
215	●	●	○	●	○	●	●	○	U8 hex.
216	●	●	○	●	○	●	●	●	U12 hex.
217	●	●	○	●	●	○	○	○	—
218	●	●	○	●	●	○	○	●	U4 hex.
219	●	●	○	●	●	○	●	○	U4 hex.
220	●	●	○	●	●	○	●	●	U8 hex.
221	●	●	○	●	●	●	○	○	U4 hex.
222	●	●	○	●	●	●	○	●	U8 hex.
223	●	●	○	●	●	●	●	○	U12 hex.
224	●	●	○	●	●	●	●	●	U12 hex.
225	●	●	●	○	○	○	○	○	—
226	●	●	●	○	○	○	○	●	U4 hex.
227	●	●	●	○	○	○	●	○	SC hex.
228	●	●	●	○	○	○	●	●	U8 hex.
229	●	●	●	○	○	●	○	○	—
230	●	●	●	○	○	●	○	●	U4 hex.
231	●	●	●	○	○	●	●	○	U4 hex.
232	●	●	●	○	○	●	●	●	U8 hex.
233	●	●	●	○	●	○	○	○	SC hex.
234	●	●	●	○	●	○	○	●	U8 hex.
235	●	●	●	○	●	○	●	○	U8 hex.
236	●	●	●	○	●	○	●	●	U12 hex.
237	●	●	●	○	●	●	○	○	U4 hex.
238	●	●	●	○	●	●	○	●	U8 hex.
239	●	●	●	○	●	●	●	○	U12 hex.
240	●	●	●	○	●	●	●	●	U12 hex.
241	●	●	●	●	○	○	○	○	JSB hex.
242	●	●	●	●	○	○	○	●	U12 hex.
243	●	●	●	●	○	○	●	○	U4 hex.
244	●	●	●	●	○	○	●	●	U12 hex.
245	●	●	●	●	○	●	○	○	U4 hex.
246	●	●	●	●	○	●	○	●	U12 hex.
247	●	●	●	●	○	●	●	○	U8 hex.
248	●	●	●	●	○	●	●	●	U12 hex.
249	●	●	●	●	●	○	○	○	U4 hex.
250	●	●	●	●	●	○	○	●	U12 hex.
251	●	●	●	●	●	○	●	○	U8 hex.
252	●	●	●	●	●	○	●	●	U12 hex.
253	●	●	●	●	●	●	○	○	U8 hex.
254	●	●	●	●	●	●	○	●	U12 hex.
255	●	●	●	●	●	●	●	○	U12 hex.
256	●	●	●	●	●	●	●	●	U12 hex.